

Functional carboxymethylcellulose/zein bionanocomposite films based on neomycin supported on sepiolite or montmorillonite clays

Ediana P. Rebitski^{a,c}, Ana C. S. Alcântara^{a,b*}, Margarita Darder^c, Rogério L. Cansian^d, Luis Gómez-Hortigüela^e and Sibele B.C. Pergher^a

^a Universidade Federal do Rio Grande do Norte, Laboratório de Peneiras Moleculares – LABPEMOL, Instituto de Química, 59078-970 Natal-RN, Brazil

^b Universidade Federal do Maranhão, Grupo de Pesquisa em Materiais Híbridos e Bionanocompósitos - Bionanos, Departamento de Química, 65080-805 São Luís-MA, Brazil

^c Instituto de Ciencia de Materiales de Madrid, CSIC, Cantoblanco, 28049 Madrid, Spain

^d Universidade Regional Integrada do Alto Uruguai e das Missões, Laboratório de Biotecnologia, 99700-000 Erechim, RS, Brazil

^e Instituto de Catálisis y Petroleoquímica, CSIC, Cantoblanco, 28049 Madrid, Spain

* Corresponding author:

e-mail: ana.alcantara@ufma.br

Phone number: +559832729243

1. Computational method details

The initial atomic coordinates of montmorillonite were taken from Viani et al.,¹ the extra-framework Ca atoms sited between the layers have been removed. All the framework atoms were kept fixed during the calculations. Periodic boundary conditions (PBC) are applied in all the calculations. Montmorillonite supercells consisting of 4x3x1 unit cells have been built in order to enable the incorporation of the large neomycin molecules within the interlaminar space (Fig. 6). This corresponds to a packing of 0.083 NMY/u.c., which is reasonably close to the experimental value of 0.065 NMY/u.c. On the other hand, atomic coordinates of sepiolite were taken from <http://icsd.iqfr.csic.es/icsd/index.php>, and the non-framework O atoms within the sepiolite channels were removed. All these framework atoms were kept fixed during the calculations. In this case, sepiolite supercells consisting of 1x1x6 unit cells have been built; approximate dimensions (calculated as interatomic distances) of the tunnels are given in Fig. 1b. For the drug model, we have used neomycin B, whose molecular structure was taken from the RCSB PDB database (NMY); all ammonium groups (6x) were studied as protonated species.

In the case of montmorillonite-neomycin hybrid, in order to compare results provided by different interatomic potentials and check the reliability of the computational settings, two general-purpose force-fields, CVFF² and Dreiding,³ have been used to model the molecular structure and the interaction energies of neomycin with the different montmorillonite frameworks. Initially, the atomic charges of the clay framework atoms were set to 1.4 and 2.4 for Al and Si, respectively, and -1.2 for O; then, in order to ensure neutrality (note that extra-framework charge-balancing cations were removed in the model), the atomic charge of Al and Si atoms were modified accordingly (uniform charge-background model) in order to provide a total net charge in the 4x3x1 supercell of -6 (which will be compensated by the incorporation of a protonated neomycin molecule). The atomic charge distribution for the organic molecule was different

depending on the force-field used. In the CVFF calculations, the neomycin charge distribution was assigned according to the CVFF force-field settings, giving a molecular charge of +6. In the calculations performed with the Dreiding force-field, the charge distribution of the neomycin molecules was obtained by the Gasteiger method,⁴ as is common for this force-field, and averaging all the charges to have a total net charge of +6. Montmorillonite frameworks with different interlayer distances (from 12.4 to 15 Å) were built by keeping the layers rigid, and varying the 'c' unit cell parameter to 12.4, 12.8, 13.2, 13.6, 14.0, 14.4 and 15.0 Å. Neomycin molecules were manually incorporated in the interlaminar space, and the systems were then geometry-optimised. In order to sample all the possible configurations, four different initial orientations of neomycin molecules (each obtained by rotating the molecule 90° around an axis perpendicular to the layer) were studied for each host-guest system. The most stable location for the neomycin molecules were obtained (for each case) by means of simulated annealing calculations (Forcite Module. BIOVIA Materials Studio 2017 R2), which consisted of heating of the system from 300 K to 500 K with temperature increments of 10 K, and then cooling to 300 K again in the same way. 250 MD steps of 1.0 fs were run in every heating/cooling step. This cycle was repeated for 20 times, and at the end of each cycle the system was geometry optimised. The stability of the different host-guest systems was calculated relative to the most stable case.

Regarding to sepiolite-neomycin hybrid material, the CVFF force-field has been used. Atomic charges of the sepiolite framework were assigned following the corresponding settings in the ClayFF forcefield,⁵ with +2.1 and +1.36 for Si and Mg atoms, respectively, and -1.06118 for all O atoms to ensure neutrality (no explicit OH⁻ groups have been included in the sepiolite model). Docking of the molecules within the sepiolite tunnels was carried out by Monte-Carlo simulations in the NVT ensemble, fixing the number of molecules to load to 1 (Sorption Module, BIOVIA Materials Studio 2017 R2). The location of the molecules was then geometry-optimised, and the most stable location for the neomycin molecules were obtained by means of simulated annealing calculations,

as before. The final interaction energies were calculated by subtracting the energy of the most stable conformation of the molecules in vacuo (obtained by simulated annealing in vacuo) to the total energy of the system; all the energy values are given in kcal/mol per neomycin molecule.

2. Hybrid material characterization

2.1 Adsorption Isotherm for Sep-Neo

Neomycin is adsorbed on sepiolite from aqueous solution of drug, as described in experimental section. The 298 K adsorption isotherm (Fig. 1) was determined from the adsorbed amounts of Neo which were deduced from the CHN elemental analysis corresponding to the different hybrid samples. The equation of the Langmuir model⁶ is expressed in equation 1:

$$r = \frac{bx_m C_s}{1+bC_s} \quad (1)$$

where r represents, in the present case, the amount of Neo adsorbed, C_s is the equilibrium concentration, x_m is the maximum amount of neomycin adsorbed and b the constant affinity between the organic adsorbate (neomycin) and the adsorbent (sepiolite). The Langmuir isotherm is identified as type C with $R = 0.9581$ and $b = 2.163 \text{ mg L}^{-1}$ which indicates the existence of good affinity between adsorbate (Neo) and adsorbent (sepiolite) (Figure S1). In addition this type of isotherm suggests that the availability of sites remains constant in all concentrations until saturation. On the other hand, the Freundlich model seems to fit better in this type of adsorption (equation 2)⁷

$$qe = K_F C_e^{1/n} \quad (2)$$

where qe is the equilibrium amount of adsorbent per unit mass of adsorbent, C_e is the concentration of neomycin at equilibrium in the aqueous solution and K_F and $1/n$ relate the adsorption capacity of the adsorbent and the intensity of the adsorption process

(parameter of heterogeneity). In this case, $n < 1$ ($n = 0.1676$) which indicates that the adsorption is favorable throughout the range of concentrations studied. In addition, the Freundlich model showed a higher correlation coefficient than the Langmuir model ($R = 0.9896$), indicating that this model seems to be more appropriate for this type of system.

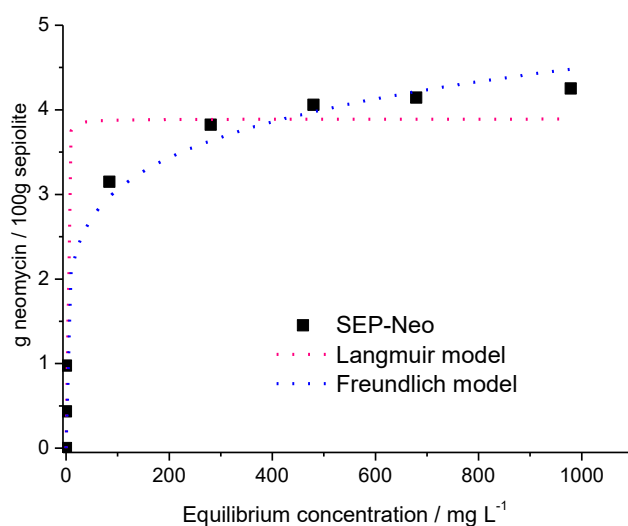


Figure S1. Adsorption isotherm at 298 K of Neo (water solutions) in sepiolite, fitting nonlinear for Langmuir and Freundlich models.

2.2 Adsorption-desorption N_2 isotherms

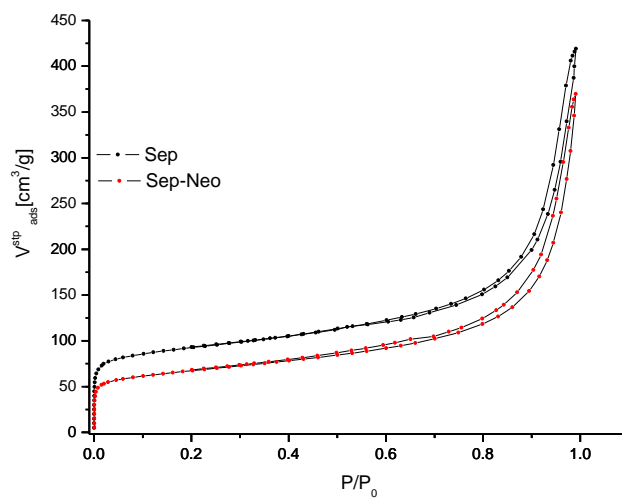


Figure S2: Adsorption-desorption N_2 isotherms obtained for pure sepiolite and Sep-Neo hybrid.

3. Computational studies

3.1 Relative energy of neomycin intercalated into montmorillonite as a function of interlayer distance

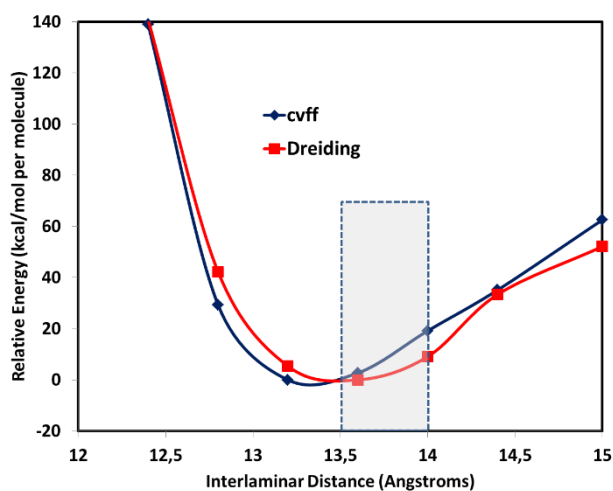


Figure S3. Relative energy (in kcal/mol per molecule) of montmorillonite (4x3x1 u.c. supercell) with one neomycin molecule loaded, as a function of the interlayer distance (defined as the 'c'

parameter), obtained using CVFF (blue) or Dreiding (red) force-fields. The experimentally observed range of interlayer distances (depending on the contact time) is displayed as a shadowed blue dashed rectangle.

3.2 Comparison of RDFs between Oext and the different H atoms of the neomycin molecules

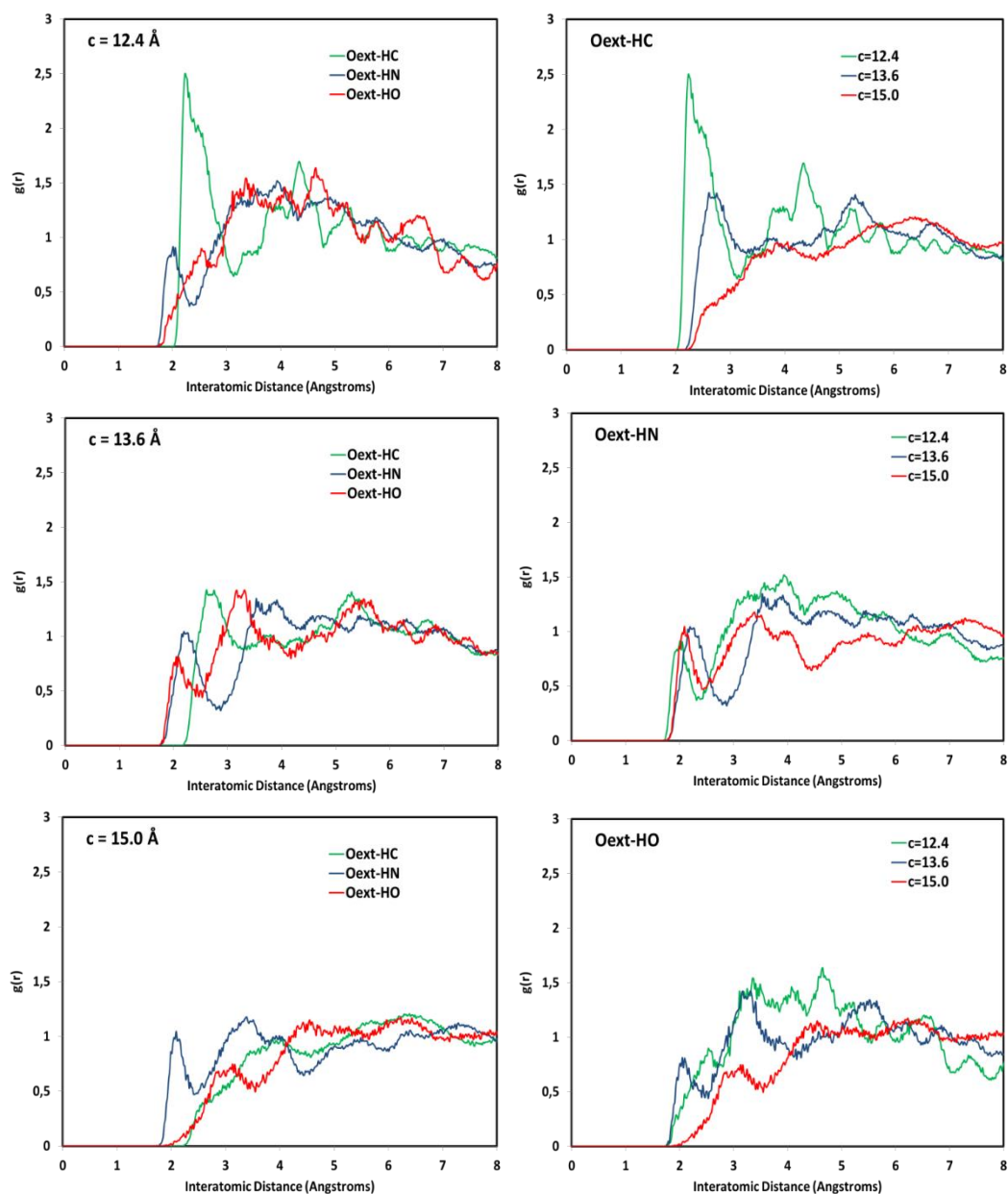


Figure S4: Comparison of RDFs between Oext (the framework O atoms in the interlayer space) and the different H atoms of the neomycin molecules occluded within montmorillonite,

distributed by systems (left: top: $c = 12.4 \text{ \AA}$; middle: $c = 13.6 \text{ \AA}$; bottom: $c = 15.0 \text{ \AA}$) or by particular RDFs (right: top: with HC; middle: with HN; bottom: with HO) for better comparison.

3.3 Simulations of the docking of planar neomycin within the sepiolite supercell

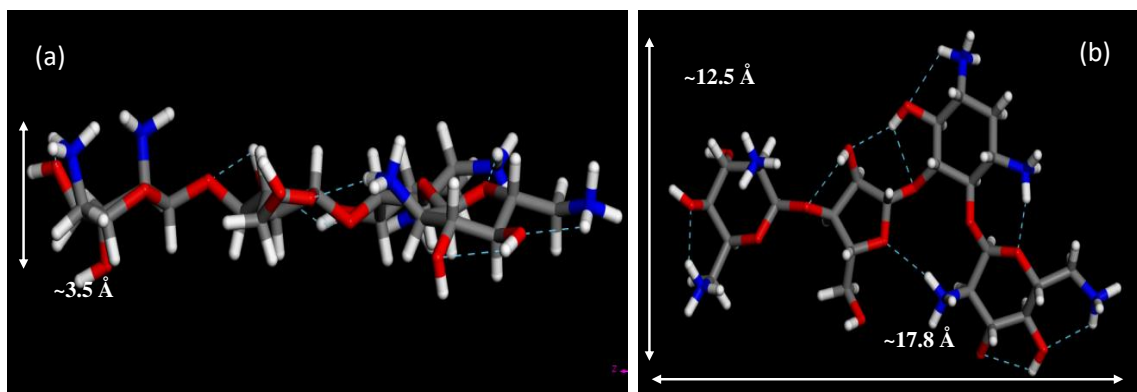


Figure S5. Dimensions of the planar molecular structure (without optimization) of neomycin used for the docking calculations: (a) height and (b) length and width.

4. Clay–neomycin based bionanocomposites films

4.1 Tensile properties

Table S1. Tensile properties of the carboxymethylcellulose-zein films. E= tensile modulus; E_b = elongation at break

Zein (%)	CMC-Z		CMC-Z/MMT-Neo		CMC-Z/Sep-Neo	
	E(GPa)	E_b (%)	E(GPa)	E_b (%)	E(GPa)	E_b (%)
0	3.72 ± 0.12	4.61 ± 1.26	4.57 ± 0.43	2.60 ± 0.22	6.25 ± 0.90	2.48 ± 0.40
10	3.08 ± 0.60	4.94 ± 0.42	4.01 ± 0.38	3.32 ± 0.85	5.87 ± 0.23	2.81 ± 0.56
50	2.36 ± 0.30	5.51 ± 0.28	3.28 ± 0.52	3.75 ± 0.63	4.64 ± 0.18	3.52 ± 0.37

4.2 Moisture-sorption isotherms

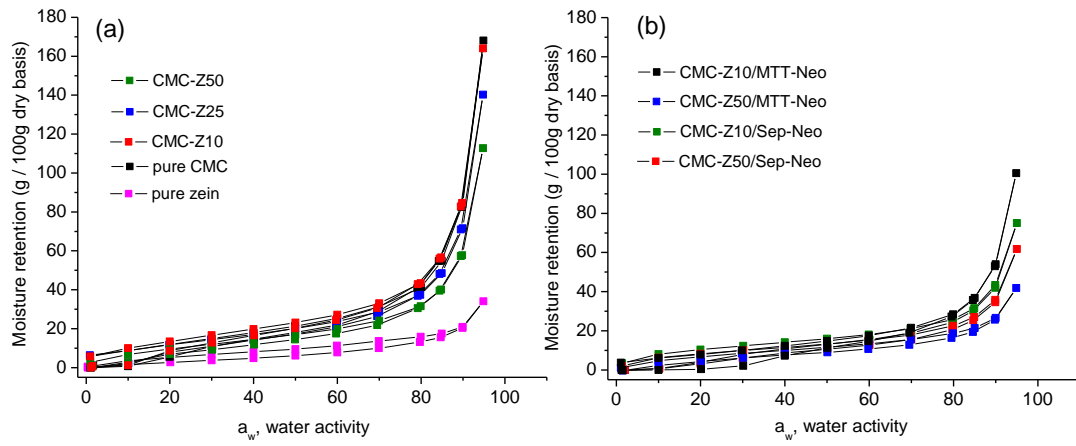


Figure S6. Moisture-sorption isotherms of (a) pure CMC and zein films and CMC-Z biopolymer films and (b) CMC-Z bionanocomposites films loaded with MMT-Neo and Sep-Neo.

4.3 Antimicrobial activity assays

Table S2: Antimicrobial activity assays for *Listeria monocytogenes*, *Staphylococcus aureus* (Gram-positive bacteria), *Escherichia coli*, *Salmonella choleraesius* (Gram-negative bacteria) versus the various bionanocomposite films that incorporate neomycin antibiotic drug: diameter of zone of inhibition (plate diffusion assay) recorded by *in vitro test*. *American Type Culture Collection

Microorganisms	CMC-Zein/Neo films			
	ATCC*	Inhibition zone (mm) 0% Zein	Inhibition zone (mm) 10% Zein	Inhibition zone (mm) 50% Zein
<i>Listeria monocytogenes</i>	7644	5.00± 0.33	5.25± 0.25	5.00± 0.38
<i>Staphylococcus aureus</i>	25923	5.25± 0.23	5.75± 0.33	5.50± 0.26
<i>Escherichia coli</i>	25922	6.00± 0.30	6.00± 0.28	6.25± 0.33
<i>Salmonella choleraesius</i>	107008	6.00± 0.27	6.25± 0.25	5.75± 0.20
CMC-Zein/MMT-Neo bionanocomposite films				
<i>Listeria monocytogenes</i>	7644	4.50± 0.24	4.50± 0.25	5.00± 0.24
<i>Staphylococcus aureus</i>	25923	4.25± 0.32	4.00± 0.33	4.25± 0.30
<i>Escherichia coli</i>	25922	4.75± 0.38	4.25± 0.33	4.25± 0.28
<i>Salmonella choleraesius</i>	107008	4.75± 0.35	5.00± 0.35	5.50± 0.33
CMC-Zein/Sep-Neo bionanocomposite films				
<i>Listeria monocytogenes</i>	7644	2.00± 0.10	2.00± 0.11	2.00± 0.10
<i>Staphylococcus aureus</i>	25923	1.00± 0.05	1.00± 0.06	1.00± 0.05
<i>Escherichia coli</i>	25922	1.50± 0.02	1.00± 0.03	1.00± 0.04
<i>Salmonella choleraesius</i>	107008	2.00± 0.10	2.00± 0.12	2.00± 0.14

REFERENCES

- (1) Viani, A.; Gualtieri A.; Artioli, G. The nature of disorder in montmorillonite by simulation of X-ray powder patterns. *Am. Mineral.* **2002**, *87*, 966-975.
- (2) Dauger-Osguthorpe, P.; Roberts, V. A.; Osguthorpe, D. J.; Wolff, J.; Genest, M.; Hagler, A. T. Structure and energetics of ligand binding to proteins: Escherichia coli dihydrofolate reductase-trimethoprim, a drug-receptor system. *Proteins: Struct., Funct., Genet.* **1988**, *4* (1), 31-47.
- (3) Mayo, S. L.; Olafson, B. D.; Goddard III, W. A. DREIDING: a generic force field for molecular simulations. *J. Phys. Chem.* **1990**, *94* (26), 8897-8909.
- (4) Gasteiger, J.; Marsili, M. Iterative partial equalization of orbital electronegativity—a rapid access to atomic charges. *Tetrahedron* **1980**, *36* (22), 3219-3228.
- (5) Cygan, R.T.; Liang, J.-J.; Kalinichev, A.G. Molecular Models of Hydroxide, Oxyhydroxide, and Clay Phases and the Development of a General Force Field. *J. Phys. Chem. B* **2004**, *108* (4), 1255-1266.
- (6) Langmuir, I. The constitution and fundamental properties of solids and liquids. II Liquids. *J. Am. Chem. Soc.* **1917**, *39*, 1848-1906.
- (7) Freundlich, H. M. F. Over the Adsorption in Solution. *J. Phys. Chem.* **1906**, *57*, 385-471.